Heliyon 9 (2023) e15872

Contents lists available at ScienceDirect

Heliyon

journal homepage: www.cell.com/heliyon

Research article

# Efficacy of puerarin in rats with focal cerebral ischemia through modulation of the SIRT1/HIF-1α/VEGF signaling pathway and its effect on synaptic plasticity

Xin Liu [a,1], Xiwen Sui [b,1], Yuqin Zhang [c], Rongchao Yue [d], Shifu Yin [e,*]

[a] Department of Internal Medicine of Traditional Chinese Medicine, The Second Affiliated Hospital of Shandong First Medical University, Taian, Shandong, China
[b] Department of Traditional Chinese Medicine, The Second People's Hospital of Dongying, Dongying, Shandong, China
[c] Department of Nursing, Binzhou Hospital of Traditional Chinese Medicine, Binzhou, Shandong, China
[d] The Second Department of Acupuncture and Moxibustion, Tai'an Hospital of Traditional Chinese Medicine, Taian, Shandong, China
[e] Department of Neurology, The People's Hospital of Gaomi, Gaomi, Shandong, China

ARTICLE INFO

*Keywords:*
Focal cerebral ischemia
Puerarin
SIRT1/HIF-1α/VEGF signaling Pathway
Synaptic plasticity
Signaling pathway

ABSTRACT

This study aimed to evaluate the efficacy of puerarin and its effect on synaptic plasticity in rats with focal cerebral ischemia (FCI) by modulating the silent mating type information regulation 2 homolog (SIRT1)/hypoxia-inducible factor-1α (HIF-1α)/vascular endothelial growth factor (VEGF) signaling pathway. Fifty specific pathogen-free-grade healthy male rats were randomly divided into sham operation group (SOG), model group, low-dose group, medium-dose group, and high-dose group, with 10 rats in each group. The SOG group received sham operation and saline treatment, while the other four groups received the same amount of saline, 25 mg/kg, 50 mg/kg, and 100 mg/kg of puerarin injection, respectively. After modeling, the rats exhibited higher neurological deficit, inflammation, cerebral infarction rate, and lower forelimb motor function as well as lower protein expressions of SIRT1, HIF-1α, VEGF, synaptophysin (SYN), and postsynaptic density protein (PSD)-95. With the treatment of different doses of puerarin, the degree of neurological impairment, impaired motor function, cerebral infarction rate, and the levels of inflammatory factors (interleukin [IL]-1β, IL-6, and intercellular adhesion molecule 1) in brain tissues were reduced; the protein expressions of SIRT1, HIF-1α, VEGF, SYN, and PSD-95 in brain tissues were enhanced, and the synaptic volume density, numerical density, surface density, width of synaptic cleft, and curvature of the synaptic interface in the cerebral cortex were also improved. Notably, the effects of puerarin on the above-mentioned indicators were dose-dependent. Puerarin can improve neurological impairment and forelimb motor function, reduce inflammatory response, inhibit brain edema, regulate synaptic plasticity, and restore the curvature of synaptic interface in rats with FCI, and its mechanism of action may be related to the activation of SIRT1/HIF-1α/VEGF signaling pathway.

* Corresponding author. Department of Neurology, The People's Hospital of Gaomi, No. 77, Zhenfu Street West, Gaomi, Shandong, 261500, China.

*E-mail addresses:* liuxin89@21cn.com (X. Liu), suixiwen@21cn.com (X. Sui), zhangyuqin5@21cn.com (Y. Zhang), yuerongchao@163.com (R. Yue), yinshifu4@21cn.com (S. Yin).

[1] Both authors contributed equally to this work and should be considered as equal first coauthors.

https://doi.org/10.1016/j.heliyon.2023.e15872
Received 4 July 2022; Received in revised form 11 April 2023; Accepted 24 April 2023
Available online 27 April 2023

## 1. Introduction

Currently, cerebrovascular disease has become a major cause of disability and mortality, with poor prognosis, high disability rate, and high morbidity [1]. Acute cerebrovascular disease, also known as stroke, is characterized by ischemic brain injury and bleeding in the brain. Approximately 80% of strokes are ischemic [2]. The irreversibility of the necrotic zone in the infarct area following cerebral ischemia causes an inflammatory response and oxidative stress, which increases the permeability of the cerebral blood-brain barrier and disrupts the integrity of the vascular endothelial cells and the tightly connected structures between brain microvascular endothelial cells, leading to an imbalance in the microenvironment of brain tissue [3,4]. It was found that endogenous revascularization can accelerate nutrient delivery and increase oxygen supply to brain tissues in ischemic areas, thus, effectively restoring functions of brain ischemic and hypoxic tissue [5]. Therefore, it is critical to induce endogenous revascularization, improve blood flow, and restore blood supply to the brain tissue in patients with ischemic cerebrovascular disease.

The process of angiogenesis is complex, mainly induced by inflammation and hypoxia, and can be regulated by many signaling pathways. The silent mating type information regulation 2 homolog (SIRT1)/hypoxia-inducible factor-1α (HIF-1α)/vascular endothelial growth factor (VEGF) signaling pathway is closely related to angiogenesis, oxidative stress response, and inflammatory response under hypoxic-ischemic conditions, and may play an active role in the mechanism of hypoxia and angiogenesis [6]. It was found that the activation of this signaling pathway helps improve resistance to oxidative stress, enhance vascular endothelial stability and endothelial remodeling, and promote neurovascular neovascularization [7]. Synaptic plasticity refers to the adaptive changes in morphology and function of synapses after neuronal damage in the brain, which is the basis for the recovery of brain neurological function; therefore, it is crucial to analyze the protective effect of drugs on focal cerebral ischemia (FCI) from the perspective of synaptic plasticity [8].

Puerarin is a vasodilator with multiple pharmacological activities, such as improving microcirculation, reducing myocardial oxygen consumption, repairing vascular endothelial cell damage, and protecting ischemic brain tissue cells [9]. Multiple studies have shown that puerarin injection can significantly promote the recovery of neurological function and improve the prognosis of patients with cerebral infarction [10]. However, the specific mechanism remains unclear. We speculated that puerarin may play a role in regulating SIRT1/HIF-1α/VEGF signaling pathway. This study was conducted to establish an FCI model using middle cerebral artery embolization and to evaluate the efficacy of puerarin on FCI rats through modulation of SIRT1/HIF-1α/VEGF signaling pathway and its effect on synaptic plasticity.

## 2. Materials and methods

### 2.1. Experimental animals

Fifty 8-week-old, specific pathogen-free (SPF)-grade healthy male rats, weighting 280–300 g were purchased from the Laboratory Animal Center of Shandong University (animal license number: SCXK [Xiang] 2019-0004). The rats were housed under the following conditions: temperature 20–25 °C, relative humidity of 65–70%, 12 h/12 h light/dark cycle, free access to water throughout the day, regular change of bedding, and the cages were cleaned and disinfected. The rats were kept for 1 week for acclimatization. The experiment complied with the relevant requirements in the Regulations of the People's Republic of China on the Administration of Laboratory Animals and approved by the Animal Ethics Committee of The People's Hospital of Gaomi (No. CYFYLL200122).

### 2.2. Main drugs, reagents, and instruments

The following drugs, reagents, and instruments were used in the study (Supplementary Table 1): puerarin injection (Xi'an Hanfeng Pharmaceutical Co., Ltd.; specification: 2 mL: 100 mg, H20033784); MCAO monofilaments (Changsha Maiyue Biotechnology Co., Ltd., China, M8500); triphenyltetrazolium chloride (TTC) staining reagent (Shanghai Jizhi Biochemical Technology Co., Ltd., China, T54930-25 g); antiSIRT1 (ab28170); antiHIF-1α (Ab1003), antiVEGF (ab10284), antisynaptophysin (SYN) (ab93133), anti-postsynaptic density protein (PSD)-95 (ab2723), secondary antibody goat antirabbit immunoglobulin G (ab7085), and antiGAPDH antibody (ab8245) (purchased from Abcam, UK); interleukin (IL)-1β enzyme-linked immunosorbent assay (ELISA) kit (Beijing Solebao Technology Co., Ltd., China, Cat. No.: SEKG-0002-96Time); IL-6 ELISA kit (Nanjing Saihongrui Biotechnology Co., Ltd., China, Cat. No.: HEA079Hu03); intercellular adhesion molecule (ICAM)-1 ELISA kit (Nanjing Sunberga Biotechnology Co., Ltd., China, Cat. No.: SBJ-H0008); Western blot electrophoresis apparatus (Bio-Rad, USA); TDZ4B-WS low-speed centrifuge (Shanghai Luxiangyi Co., Ltd., China); Image-ProPlus 6.0 image analysis system (Media Cybernetics Co., Ltd., USA); and transmission electron microscope (Huison Biotechnology [Shanghai] Co., Ltd., China).

## 3. Methods

### 3.1. Modeling

Forty SPF healthy male rats (8 weeks of age, body mass 280–300 g) fasted overnight but were allowed to drink freely. According to the methods provided by Horn [11] and Zhang et al. [12], the model of FCI in rats were prepared by the middle cerebral artery embolization as following procedures: the rats were anesthetized via an intraperitoneal injection of 2% sodium pentobarbital, placed in the right lateral position, fixed on the operating table, and the skin was cut with surgical scissors along the midpoint of the line

between the ears and eyes of the rat. The internal carotid artery, vagus nerve, right carotid artery, and external carotid artery were separated, and the distal end of the external carotid artery was double ligated with a thin thread, and then cut-off at the proximal end of the branch of the tongue and maxillary artery. A small incision was made, and sutures were inserted into the stumps of the external and internal carotid arteries, and the cerebral blood flow was occluded for 60 min after ≥70% under the laser Doppler flow monitor. In the sham operation group (SOG), except for the insertion of nylon thread, the sham operation was the same as the above procedure, that is, only the internal and external carotid arteries and the common carotid artery were separated, and the skin was sutured.

### 3.2. Grouping and treatments

Fifty SPF-grade healthy male rats were randomly divided into the SOG, model group (MG), low-dose group (LDG), medium-dose group (MDG), and high-dose group (HDG). Puerarin stock solution was prepared in water containing 0.5%CMC-Na (m/v). In the dose-response study, puerarin was administered at 25, 50 and 100 mg/kg, respectively. All the treatments or vehicle were randomly given by gavage 1 h after MCAO. In order to study the long-term protective effect of puerarin on rats, each group was given puerarin by continuous gavage. Among them, 25, 50 and 100 mg/kg of puerarin were injected into the tail vein of the LDG, MDG, and HDG, respectively, and an equal amount of saline was injected into the tail vein of the SOG and MG, and the drug was administered repeatedly for 7 days.

### 3.3. Neurological function score

At 12 h postoperatively (before treatment), 48 h postoperatively (after treatment), and 7 days postoperatively (at the end of treatment), the neurological function of the rats was assessed based on Bederson 5-point scale as described previously [13]: no symptoms of neurological deficit was scored as 0, inability to fully extend the upper limb on the contralateral side of surgery was scored as 1, reduced resistance when pushing to the contralateral side was scored as 2, turning to the contralateral side when lifting the tail was scored as 3, automatic turning when walking was scored as 4, and no spontaneous activity, loss of consciousness, and no response to stimulation were scored as 5 points. The score of neurological performance was conducted by a strictly trained experimenter who was blind to the treatment, so as to avoid the influence of subjective factors on the experimental results.

### 3.4. Forelimb motor function score

At 12 h, 48 h, and 7 days postoperatively, Montoya's staircase test was modified as reported previously [14]. There were seven staircases on each side of the transparent glass resin box, three food balls were placed in the food trough of each staircase, the rats were placed inside the box, and the forelimb motor function score was evaluated as the number of food balls grasped by the forelimb within 15 min. The score of forelimb motor function was conducted by a strictly trained experimenter who was blind to the treatment, so as to avoid the influence of subjective factors on the experimental results.

### 3.5. Cerebral infarction rate

After 7 days of continuous administration, five rats in each group were randomly sacrificed using intraperitoneal anesthesia, and their brains were removed by severing their heads and placed in a freezer at −20 °C for 30 min. After removal, the brains of rats were routinely sectioned along the coronal plane of 2 mm and placed in 2% TTC solution at 37 °C under light-proof conditions for 30 min. After staining, the infarcted area of the brain was white and the noninfarcted area was red. The cerebral infarct area was calculated using Image-ProPlus 6.0 image analysis system, and the size of infarct area/brain area at the ischemic side × 100% was equal to the percentage of cerebral infarct area on the ischemic side.

### 3.6. Brain tissue-related protein expression

Brain tissue was extracted and weighed, and normal saline was added to prepare 10% tissue homogenate as described previously [15]. The tissue homogenate was centrifuged at 3000 rpm for 15 min at 4 °C, and the supernatant was taken and stored at −20 °C. The supernatant was taken and quantified using the BCA method. An equal amount of protein sample was extracted, denatured at 100 °C for 5 min, followed by 12% sodium dodecyl sulphate-polyacrylamide gel electrophoresis, polyvinylidene fluoride membrane transfer, and blocking with 5% bovine serum albumin at room temperature for 2 h, and the corresponding primary antibody (1:1000 dilution) was added. After washing with TBST, the secondary antibody goat antirabbit immunoglobulin G (1:2000 dilution) was added, and the membrane was incubated at room temperature for 1.5 h, washing with TBST. Proteins were visualized using enhanced chemiluminescence luminescence reagent, and quantitative analysis was performed using Image J software. GAPDH (1:1000 dilution) was used as an internal reference, and the ratio indicated the relative content of the target protein.

### 3.7. Inflammatory factors

The brain homogenate was taken, centrifuged at high speed and low temperature, and the supernatant was collected. The levels of IL-1β, IL-6, and ICAM-1 were determined using ELISA. Standard and sample diluent was added to the blank well, and the corresponding samples were added to the rest of the corresponding wells. The reaction wells were sealed with a sealing tape and incubated

in an incubator at 36 °C for 90 min. The biotinylated antibody working solution was prepared 20 min in advance, and the plates were washed five times. The blank well was added with biotinylated antibody diluent, and the remaining wells were added with biotinylated antibody working solution (100 μL/well). The reaction wells were sealed with a new plate-sealing tape and incubated in an incubator at 36 °C for 60 min. The enzyme conjugate working solution was prepared 20 min in advance and stored at room temperature (22–25 °C) away from light, and the plate was washed five times. The blank well was added with enzyme conjugate diluent, and the remaining wells were added with enzyme conjugate working solution (100 μL/well). The reaction wells were sealed with a new plate-sealing tape and incubated in an incubator at 36 °C for 30 min in the dark. The microplate reader was turned on and preheated, and the detection program was set up. The plate was washed five times. The color substrate (TMB) was added (100 μL/well) and incubated in an incubator at 36 °C for 15 min in the dark. The stop solution (100 μL/well) was added, and the optical density value at 450 nm was measured immediately after mixing (within 3 min).

### 3.8. Brain cortical synaptic ultramorphology

At the end of drug administration in the remaining five rats, 2% sodium pentobarbital was injected intraperitoneally for anesthesia, and the chest was opened, exposing the heart. The left ventricle aorta was cannulated, and saline at 37 °C was instilled at a dose of 100 mL and perfused with phosphate buffer saline (PBS) for 30 min. The left ischemic rat cerebral cortex was taken and partially placed in PBS solution for fixation, rinsed three times with PBS after 3 h, eluted with gradient ethanol, dehydrated with acetone, permeabilized for 2 h and 3 h in each containing acetone embedding solution and pure Epon812 embedding solution, placed in an oven at a temperature of 60 °C overnight, and routinely sectioned to a thickness of approximately 60 nm. The sections were placed on a copper grid, stained with uranyl acetate and lead citrate, and the synaptic ultrastructure of the cerebral cortex area was observed under transmission electron microscopy. The ultrastructure of synapses was observed by electron microscopy, and the numerical density (Nv), synaptic volume density (Vv), and surface density (Sv) were quantitatively analyzed according to Bertoni-Freddari et al. [16] The width of the synaptic cleft and the curvature of the synaptic interface were quantitatively analyzed by bioimaging analyzer.

### 3.9. Statistical analysis

Statistical package for the social sciences 24.0 statistical analysis software was used, and the measurement data conforming to the normal distribution were expressed as mean ± standard deviation while one-way analysis of variance was used for comparison between multiple groups, and Newman–Keuls test was used for further two-by-two comparisons. $P < 0.05$ was considered statistically significant.

## 4. Results

### 4.1. Neurological deficit scores

The neurological deficit scores at 12 h, 48 h, and 7 days postoperatively were higher in the MG than in the SOG (P < 0.05). The

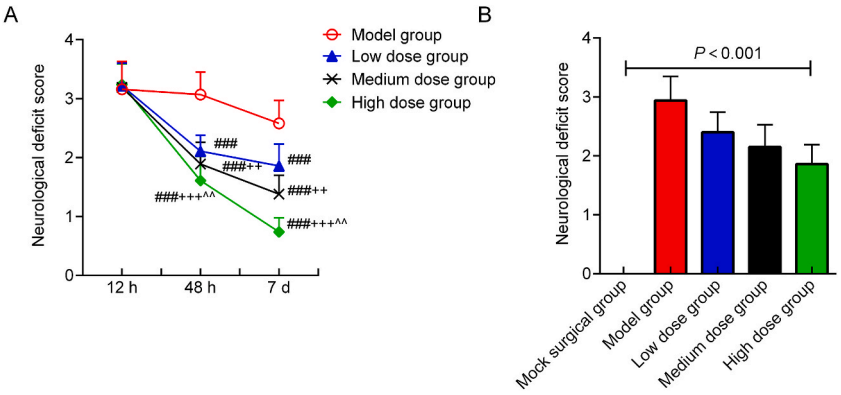


**Fig. 1.** Comparison of neurological deficit scores (n = 5)
Fig. 1 shows obvious neurological impairment in rats with focal cerebral ischemia, and puerarin can reduce the degree of neurological impairment in a dose-dependent manner. A: One-way analysis of variance showed that there was a statistically significant difference between groups at 12 h postoperatively (F = 165.019, df = 4, P = 0.000), and analysis of covariance showed that there was a statistically significant difference between groups at 48 h postoperatively (F = 53.669, df = 4, P = 0.000) and 7 d postoperatively (F = 81.014, df = 4, P = 0.000). B: A two-way ANOVA with repeated measures was conducted, and the results showed that the neurological deficit score was statistically significant between the groups ($P < 0.001$). Note: Compared with the model group, $^{\#\#\#}P < 0.001$; compared with the low-dose group, $^{++}P<0.01$, $^{+++}P<0.001$; compared with the medium-dose group, $^{\wedge\wedge}P < 0.01$. Low-dose group: 25 mg/kg of puerarin; medium-dose group: 50 mg/kg of puerarin; high-dose group: 100 mg/kg of puerarin.

neurological deficit scores at 48 h and 7 days postoperatively in the HDG < MDG < MG ($P < 0.05$), indicating that rats with FCI had significant neurological deficits, and puerarin could reduce the degree of neurological impairment in a dose-dependent manner (Fig. 1A and B).

### 4.2. Motor function of the left forelimb

The motor function scores of the left forelimb at 12 h, 48 h, and 7 days after surgery in the MG were lower than those in the SOG ($P < 0.05$). The motor function scores of the left forelimb at 48 h and 7 days after surgery in the HDG > MDG > LDG > MG ($P < 0.05$), indicating that puerarin could reduce the impaired motor function of the left forelimb in rats with FCI in a dose-dependent manner (Fig. 2A and B).

### 4.3. Cerebral infarction rate

The cerebral infarction rate in the MG was higher than that in the SOG ($P < 0.05$). The cerebral infarction rate in the HDG < MDG < LDG < MG ($P < 0.05$), indicating that puerarin could reduce the cerebral infarction rate in rats with FCI in a dose-dependent manner (Fig. 3).

### 4.4. SIRT1/HIF-1α/VEGF signaling pathway-related protein expression in brain tissue

SIRT1, HIF-1α, and VEGF protein expression in brain tissue of the MG was lower than that of the SOG ($P < 0.05$) (Fig. 4A); SIRT1 (Fig. 4B), HIF-1α (Fig. 4C), and VEGF (Fig. 4D) protein expression in brain tissue of HDG > MDG > LDG > MG ($P < 0.05$) (Supplementary Fig. 1), indicating that puerarin could activate SIRT1/HIF-1α/VEGF signaling pathway in brain tissue of rats with FCI in a dose-dependent manner.

### 4.5. Expression of synaptic plasticity-related proteins in brain tissues

The expression of SYN and PSD-95 in the brain tissue of the MG was lower than that of the SOG ($P < 0.05$) (Fig. 5A). The expression of SYN (Fig. 5B) and PSD-95 (Fig. 5C) in the brain tissue of the HDG > MDG > LDG > MG ($P < 0.05$) (Supplementary Fig. 2), indicating that puerarin could enhance the expression of SYN and PSD-95 in the brain tissue of rats with FCI and improve synaptic plasticity in brain tissue in a dose-dependent manner.

### 4.6. Mitochondrial morphological structure of nerve cells in rat brain tissue

Mitochondrial morphology and structure of cortical nerve cells in the SOG were normal (Fig. 6A). Compared with the SOG, the mitochondria of cortical nerve cells on the ischemic side of the MG were severely damaged, with atrophy of morphological structures, increased mitochondrial membrane density, and significantly reduced or absent cristae, and typical ferroptosis (Fig. 6B). Compared

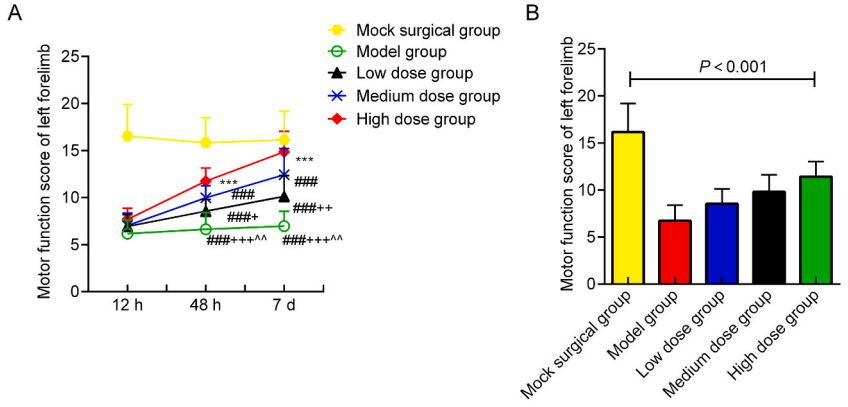


**Fig. 2.** Comparison of motor function scores of the left forelimb (n = 5)
Puerarin can alleviate motor impairment of left forelimb in rats with focal cerebral ischemia in a dose-dependent manner. A: One-way analysis of variance showed that there was a statistically significant difference between the groups in motor function scores of left forelimb 12 h postoperatively ($F = 51.179$, $df = 4$, $P = 0.000$), and analysis of covariance showed that there was a statistically significant difference between groups at 48 h postoperatively ($F = 25.204$, $df = 4$, $P = 0.000$) and 7 d postoperatively ($F = 24.882$, $df = 4$, $P = 0.000$). B: A two-way ANOVA with repeated measures was conducted, and the results showed that motor function score of left forelimb was significantly different between the groups ($F = 81.104$, $df = 4$, $P = 0.000$). Note: Compared with the sham operation group, $^{***}P < 0.001$; compared with the model group, $^{\#\#\#}P < 0.001$; compared with the low-dose group, $^{+}P<0.05$, $^{++}P<0.01$, $^{+++}P<0.001$; compared with the medium-dose group, $^{\wedge\wedge}P < 0.01$. Low-dose group: 25 mg/kg of puerarin; medium-dose group: 50 mg/kg of puerarin; high-dose group: 100 mg/kg of puerarin.

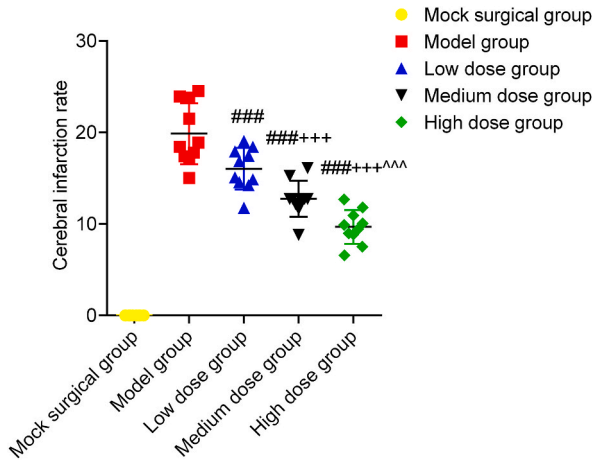


**Fig. 3.** Comparison of cerebral infarction rate (n = 5)
Puerarin can reduce the rate of cerebral infarction in rats with focal cerebral ischemia in a dose-dependent manner. There were significant differences in cerebral infarction rates among all groups (F = 120.297, df = 4, P = 0.000). Note: Compared with the model group, $^{###}P < 0.001$; compared with the low-dose group, $^{+++}P<0.001$; compared with the medium-dose group, $^{\wedge\wedge\wedge}P < 0.001$. Low-dose group: 25 mg/kg of puerarin; medium-dose group: 50 mg/kg of puerarin; high-dose group: 100 mg/kg of puerarin.

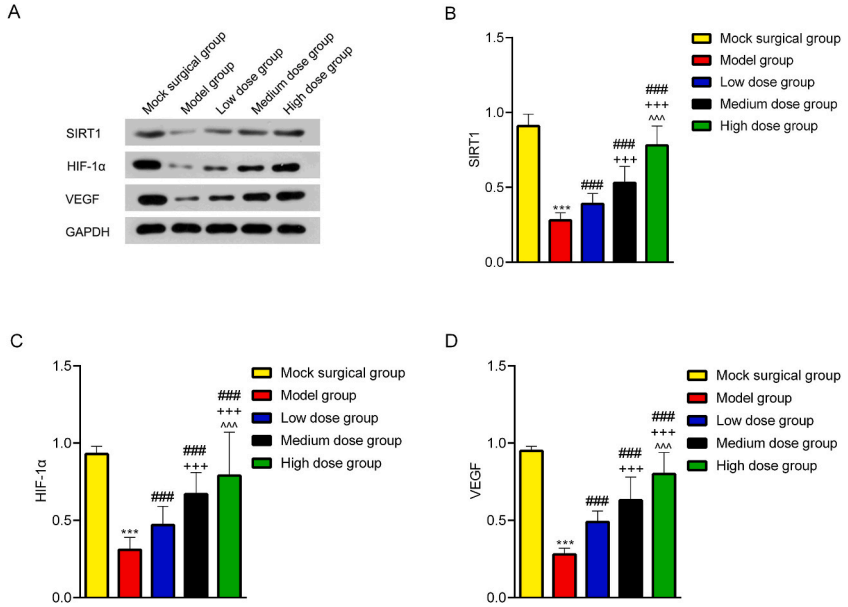


**Fig. 4.** Comparison of SIRT1/HIF-1α/VEGF signaling pathway-related protein expression (n = 5)
Puerarin can activate the expression of (A) SIRT1, (B) HIF-1α and (C) VEGF protein in the brain tissue of focal cerebral ischemia rats in a dose-dependent manner. One-way analysis of variance showed that there were statistically significant differences in the expression of (A) SIRT1, (B) HIF-1α and (C) VEGF protein in brain tissues of all groups (SIRT1: F = 40.514, df = 4, P = 0.000; HIF-1α: F = 12.479, df = 4, P = 0.000; VEGF = 33.801, df = 4, P = 0.000). SIRT1: silent mating type information regulation 2 homolog, HIF-1α: hypoxia-inducible factor-1α, VEGF: vascular endothelial growth factor. Note: Compared with the sham operation group, $^{***}P < 0.001$; compared with the model group, $^{###}P < 0.001$; compared with the low-dose group, $^{+++}P<0.001$; compared with the medium-dose group, $^{\wedge\wedge\wedge}P < 0.001$. Low-dose group: 25 mg/kg of puerarin; medium-dose group: 50 mg/kg of puerarin; high-dose group: 100 mg/kg of puerarin.

with the MG, the mitochondrial structure of rat nerve cells in the HDG of puerarin was significantly improved, with mild damage, normalized morphology, reduced membrane density and increased number of cristae (Fig. 6C).

### *4.7. Synaptic morphometric analysis*

The synaptic Vv, Nv, Sv, width of the synaptic cleft, and curvature of the synaptic interface in the cerebral cortex of the MG were

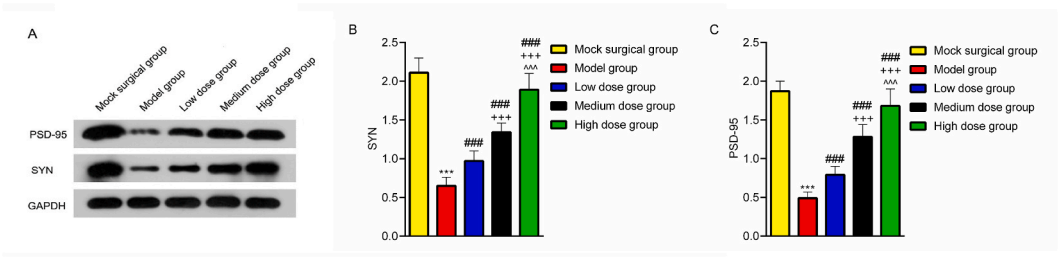


**Fig. 5.** Comparison of synaptic plasticity-related protein expressions (n = 5)
Puerarin elevated (A) SYN and (B) PSD-95 protein expression in brain tissue of rats with focal cerebral ischemia and improved synaptic plasticity in brain tissue in a dose-dependent manner. One-way analysis of variance showed that there were significant differences in expression of (A) SYN and (B) PSD-95 protein in brain tissues of each group (SYN: F = 77.559, df = 4, P = 0.000; PSD-95: F = 76.981, df = 4, P = 0.000). SYN: synaptophysin, PSD-95: postsynaptic density protein-95. Note: Compared with the sham operation group, ***P < 0.001; compared with the model group, $^{\#\#\#}$P < 0.001; compared with the low-dose group, $^{+++}$P<0.001; compared with the medium-dose group, $^{\wedge\wedge\wedge}$P < 0.001. Low-dose group: 25 mg/kg of puerarin; medium-dose group: 50 mg/kg of puerarin; high-dose group: 100 mg/kg of puerarin.

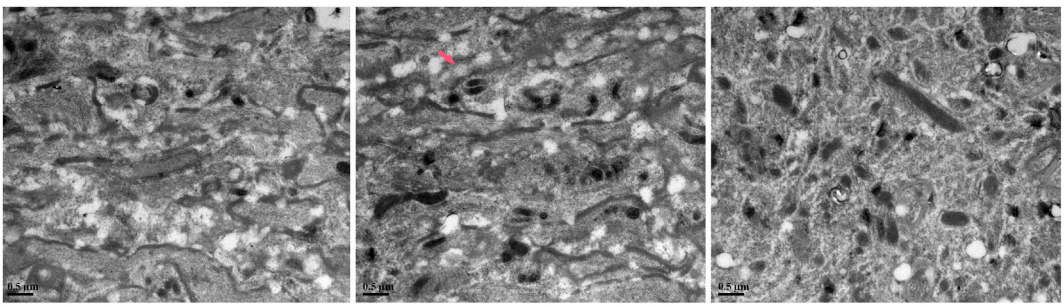


**Fig. 6.** The ultrastructure of synapses in cerebral cortex under transmission electron microscope.
Note: A: sham operation group; B: model group; C: puerarin high-dose group.

lower than those of the SOG (P < 0.05). The synaptic Vv, Nv, Sv, width of synaptic cleft, and curvature of the synaptic interface in the cerebral cortex in HDG > MDG > LDG > MG (P < 0.05), indicating that puerarin could restore the curvature of synaptic interface and protect synaptic plasticity in a dose-dependent manner (Table 1).

### *4.8. Inflammatory factors*

The levels of IL-1β, IL-6, and ICAM-1 in brain tissues of the MG were higher than those of the SOG (P < 0.05). The levels of IL-1β, IL-6, and ICAM-1 in brain tissues of the HDG < MDG < LDG < MG (P < 0.05), indicating that puerarin could reduce the inflammatory response in a dose-dependent manner (Table 2).

**Table 1**
Comparison of morphometric analysis of synaptic morphology in cortical areas ($\bar{\chi}\pm$S) (n = 5).

| Group | Number of cases | Vv (μm2/μm3) | Nv (piece/μm3) | Sv (μm2/μm3) | Width of synaptic cleft (nm) | Synaptic interface curvature |
|---|---|---|---|---|---|---|
| Sham operation group | 5 | 0.14 ± 0.03 | 2.35 ± 0.12 | 0.15 ± 0.03 | 25.98 ± 2.24 | 1.29 ± 0.05 |
| Model group | 5 | 0.04 ± 0.01*** | 0.39 ± 0.07*** | 0.04 ± 0.01*** | 13.74 ± 3.36*** | 0.91 ± 0.04*** |
| Low dose group | 5 | 0.08 ± 0.02$^{\#\#\#}$ | 0.98 ± 0.13$^{\#\#\#}$ | 0.07 ± 0.01$^{\#\#\#}$ | 16.28 ± 3.16$^{\#\#\#}$ | 1.08 ± 0.05$^{\#\#\#}$ |
| Medium dose group | 5 | 0.11 ± 0.02$^{\#\#\#++}$ | 1.35 ± 0.15$^{\#\#\#+++}$ | 0.10 ± 0.03$^{\#\#\#+++}$ | 20.39 ± 4.25$^{\#\#\#+++}$ | 1.18 ± 0.07$^{\#\#\#+++}$ |
| High dose group | 5 | 0.13 ± 0.02$^{\#\#\#+++\wedge}$ | 1.98 ± 0.24$^{\#\#\#+++\wedge\wedge}$ | 0.13 ± 0.05$^{\#\#\#+++\wedge\wedge\wedge}$ | 23.95 ± 4.73$^{\#\#\#+++\wedge\wedge\wedge}$ | 1.25 ± 0.11$^{\#\#\#+++\wedge\wedge\wedge}$ |
| F/P | | 16.756/0.000 | 145.695/0.000 | 10.134/0.000 | 9.778/0.000 | 24.465/0.000 |

Note: One-way analysis of variance showed that there were statistically significant differences in Vv, Nv, Sv, width of synaptic cleft and synaptic interface curvature in brain tissues of all groups (Vv: F = 16.756, df = 4, P = 0.000; Nv: F = 145.695, df = 4, P = 0.000; Sv: F = 10.134, df = 4, P = 0.000; width of synaptic cleft: F = 9.778, df = 4, P = 0.000; synaptic interface curvature: F = 24.465, df = 4, P = 0.000). Compared to the sham operation group, ***P < 0.05; compared to the model group, $^{\#\#\#}$P < 0.001; compared to the low-dose group, $^{++}$P < 0.01, $^{+++}$P < 0.001; compared to the medium-dose group, $^{\wedge}$P < 0.05, $^{\wedge\wedge}$P < 0.01, $^{\wedge\wedge\wedge}$P < 0.001. Vv: volume density, Nv: numerical density, Sv: surface density.

## 5. Discussion

Puerarin, chemically known as 4,7-dihydroxy-8-*d*-glucosyl isoflavone, scavenges free radicals, is an antioxidant, and improves the microcirculation [17]. Researchers found that puerarin pretreatment could protect mitochondrial function and reduce the water content of brain tissue by reducing oxidative stress-related injury, inhibiting brain edema, enhancing the antioxidant capacity of brain tissue, and reducing lipid peroxidation, thus alleviating neurological function in rats with FCI-reperfusion injury [18]. Zhang et al. [19] reported that puerarin could play a role in attenuating neurological deficits by regulating the Bcl-2/Bax/cleaved caspase-3 and Sirt3/SOD2 apoptotic pathways. Zhao et al. [20] showed that puerarin could improve blood-brain barrier permeability and attenuate cerebral ischemia-reperfusion injury. In this study, an FCI model was established through middle cerebral artery embolization, and the results showed that the neurological deficit score and motor function score of the left forelimb in the MG at 12 h postoperatively (before treatment) were higher than those in the SOG, which showed that the rat model of FCI was successfully established, and the rats were accompanied by neurological and motor deficits of the left forelimb. The rats showed improved neurological deficit score and motor function score of left forelimb and low cerebral infarction rate and reduced tissue levels of IL-1β, IL-6, and ICAM-1, suggesting that puerarin could improve neurological and limb functions, reduce inflammatory response, and shrink cerebral infarction area in rats with FCI, similar to the results of the above study.

SIRT1 is a type III histone deacetylase that interacts with many crucial transcriptional coregulators and transcription factors and can regulate chromosome stability, gene transcription, and target protein activity under deacetylation, thus participating in oxidative stress, energy metabolism, and other processes related to hypoxia-ischemia [21]. Also, SIRT1 is a key regulator in the angiogenic response, helping promote endothelial remodeling and improve vascular endothelial stability. HIF-1α is a subunit of the nuclear protein HIF-1, and its upregulation can play a key role in the hypoxic stress response by enhancing the transcription of hypoxia-responsive genes, such as adrenomedullin, erythropoietin, and endothelin. VEGF is a major regulator of angiogenesis and has many biological effects, such as stimulating endothelial cell differentiation, increasing vascular permeability, inhibiting apoptosis of mature dendritic cells and endothelial cells, promoting differentiation and migration of endothelial cells, and mediating angiogenesis [22]. It was found that hypoxic-ischemic conditions are potent triggers of VEGF transcription [23]. Mi et al. [24] showed that activation of the SIRT1/HIF-1α/VEGF signaling pathway protects against hypoxia/high glucose-induced proliferation and migratory injury in cerebral microvascular endothelial cells. Geng et al. [25] found that the upregulation of HIF-1α/VEGF signaling pathway-related protein expression improved mouse skin flap ischemia-reperfusion injury, improved the hypoxia tolerance of human umbilical vein endothelial cells, and maintained vascular homeostasis. Ruan et al. [26] found that the activation of the SIRT1/HIF-1α/VEGF signaling pathway alleviated brain injury after cerebral ischemia-reperfusion and promoted angiogenesis in cerebral microvascular endothelial cells. In this study, we found that SIRT1, HIF-1α, and VEGF protein expression in brain tissues of the HDG > MDG > LDG > MG, indicating that the mechanism of puerarin in reducing the degree of neurological deficits and shrinking the area of cerebral infarction in rats with FCI may be related to the activation of SIRT1/HIF-1α/VEGF signaling pathway, and the effect was dose-dependent.

Synaptic plasticity is the plasticity basis of the cortex related to the recovery of motor function and sensory and memory impairments. Changes in the synaptic structure and number can affect brain neurotransmission. Excitotoxic effects of excitatory amino acids occur after FCI, which disrupt the balance of inhibitory and excitatory synaptic plasticity in neurons, reducing the efficiency of information generation, transmission, and behavioral adaptation in the brain, causing a decrease in the number of synapses and weakening synaptic plasticity [27]. SYN is a calcium-binding protein on the membrane of synaptic vesicles, and its expression is related to neurotransmitter release and synaptic density. PSD-95 is an ultrastructure attached to the cytoplasmic side of the postsynaptic membrane, and is associated with the regulation of synaptic activity, ion channel function, and intracellular signal transduction [28]. Zhao et al. [29] found that the expression of SYN protein in neurons in the CA1 region of the rat hippocampus decreased within 3 days following cerebral ischemia-reperfusion injury and showed an increasing trend after 3 days, peaking at the 14th day. Lei et al. [30] found that neuronal PSD-95 protein expression was downregulated in the CA1 region of the rat hippocampus after cerebral ischemia-reperfusion injury, whereas upregulation of PSD-95 expression protected neurological function and enhanced synaptic plasticity. In this study, SYN; PSD-95 protein expression; synaptic Vv, Nv, and Sv; width of the synaptic cleft; and synaptic interface curvature in the MG were lower than those in the SOG, indicating that the width of the synaptic cleft was significantly narrower, fewer in number, and shorter in the connecting bands, while the synaptic interface curvature was reduced, and synaptic structure, number, and morphology were changed in rats with FCI. The expression of SYN; PSD-95 protein; synaptic Vv, Nv, and Sv; width of the synaptic cleft; and synaptic interface curvature in the cortical area of rats increased after treatment with puerarin, which showed that puerarin could restore synaptic interface curvature, protect synaptic plasticity, and promote synaptic development, and the most optimal effect was achieved at high doses. Li et al. [31] found that after treatment of puerarin in rats with cerebral ischemia-reperfusion, the synapses of the puerarin group became dense; concave synapses were increased, usually with two active sites; the postsynaptic density was thickened; and the gap was clear. The curvature of the synaptic interface in the penumbra of the affected cortex was increased, the postsynaptic density was thickened, and the synaptic gap was reduced; the morphological and structural parameters of the synapses in the 7-days and 14-days groups were better than those in the model group, which is consistent with the results of the present study. It is suggested that the modulation of synaptic plasticity in the brain tissue by puerarin may be an important mechanism to promote neurological recovery in patients with cerebral infarction.

In summary, puerarin can reduce neurological impairment, improve forelimb motor function, reduce inflammatory response, inhibit brain edema, regulate synaptic plasticity in brain tissue, and restore synaptic interface curvature in rats with FCI. Moreover, its mechanism of action may be related to the activation of SIRT1/HIF-1α/VEGF signaling pathway. This study provides an intuitive morphological basis for elucidating the role of puerarin in promoting neural function and synaptic plasticity repair after FCI; however,

**Table 2**
Comparison of inflammatory factor levels in brain tissue of rats ($\bar{\chi}\pm S$, pg/mg) (n = 5).

| Group | Number of cases | IL-1β | IL-6 | ICAM-1 |
|---|---|---|---|---|
| Sham operation group | 5 | 2.32 ± 0.42 | 20.36 ± 3.25 | 17.67 ± 4.64 |
| Model group | 5 | 7.59 ± 1.21*** | 31.68 ± 4.85*** | 28.34 ± 3.97*** |
| Low dose group | 5 | 6.01 ± 0.93### | 27.13 ± 3.35### | 24.74 ± 2.38### |
| Medium dose group | 5 | 4.43 ± 0.84###+++ | 24.02 ± 2.37###+++ | 21.16 ± 2.11###+++ |
| High dose group | 5 | 3.02 ± 0.75###+++^^^ | 21.11 ± 3.38###+++^^^ | 18.10 ± 3.35###+++^^^ |
| F/P | | 30.680/0.000 | 8.685/0.000 | 8.792/0.000 |

Note: One-way analysis of variance showed that there were statistically significant differences in the levels of IL-1β, IL-6 and ICAM-1 in the brain tissues of all groups (IL-1β: F = 30.680, df = 4, P = 0.000; IL-6: F = 8.685, df = 4, P = 0.000; ICAM-1: F = 8.792, df = 4, P = 0.000). Compared with the sham operation group, ***P < 0.05; compared with the model group, ###P < 0.001; compared with the low-dose group, +++P<0.001; compared with the medium-dose group, ^^^P < 0.001. IL-1β: interleukin-1β, IL-6: interleukin-6, ICAM-1: intercellular adhesion molecule-1.

due to financial reasons, only the structural images of the SOG, MG and HDG of puerarin were taken under electron microscope, which requires further observation and analysis in the next study, and its specific mechanism of action and its relationship with SIRT1/HIF-1α/VEGF signaling pathway need further investigation.

## Funding

This research did not receive any specific grant from funding agencies in the public, commercial, or not-for-profit sectors.

## Author contribution statement

Xiwen Sui; Shifu Yin: Conceived and designed the experiments; Contributed reagents, materials, analysis tools or data; Wrote the paper.

Xin Liu: Conceived and designed the experiments; Performed the experiments.

Yuqin Zhang; Rongchao Yue: Performed the experiments; Analyzed and interpreted the data.

## Data availability statement

Data will be made available on request.

## Declaration of competing interest

The authors declare that they have no known competing financial interests or personal relationships that could have appeared to influence the work reported in this paper.

## Appendix ASupplementary data

Supplementary data to this article can be found online at https://doi.org/10.1016/j.heliyon.2023.e15872.

## References

[1] L.B. Goldstein, Introduction for focused updates in cerebrovascular disease, Stroke 51 (3) (2020) 708–710, https://doi.org/10.1161/STROKEAHA.119.024159.
[2] C.D. Maida, R.L. Norrito, M. Daidone, A. Tuttolomondo, A. Pinto, Neuroinflammatory mechanisms in ischemic stroke: focus on cardioembolic stroke, background, and therapeutic approaches, Int. J. Mol. Sci. 21 (18) (2020) 6454, https://doi.org/10.3390/ijms21186454.
[3] S. Paul, E. Candelario-Jalil, Emerging neuroprotective strategies for the treatment of ischemic stroke: an overview of clinical and preclinical studies, Exp. Neurol. 335 (2021), 113518, https://doi.org/10.1016/j.expneurol.2020.113518.
[4] X.T. Su, L. Wang, S.M. Ma, Y. Cao, N.N. Yang, L.L. Lin, M. Fisher, J.W. Yang, C.Z. Liu, Mechanisms of acupuncture in the regulation of oxidative stress in treating ischemic stroke, Oxid. Med. Cell. Longev. 2020 (2020), 7875396, https://doi.org/10.1155/2020/7875396.
[5] M. Hatakeyama, I. Ninomiya, M. Kanazawa, Angiogenesis and neuronal remodeling after ischemic stroke, Neural Regen. Res. 15 (1) (2020) 16–19, https://doi.org/10.4103/1673-5374.264442.
[6] H. Zhang, S. He, C. Spee, K. Ishikawa, D.R. Hinton, SIRT1 mediated inhibition of VEGF/VEGFR2 signaling by resveratrol and its relevance to choroidal neovascularization, Cytokine 76 (2) (2015) 549–552, https://doi.org/10.1016/j.cyto.2015.06.019.
[7] Y. Lin, L. Li, J. Liu, X. Zhao, J. Ye, P.S. Reinach, J. Qu, D. Yan, SIRT1 deletion impairs retinal endothelial cell migration through downregulation of VEGF-A/VEGFR-2 and MMP14, Invest. Ophthalmol. Vis. Sci. 59 (13) (2018) 5431–5440, https://doi.org/10.1167/iovs.17-23558.
[8] N.V. Luchkina, V.Y. Bolshakov, Mechanisms of fear learning and extinction: synaptic plasticity-fear memory connection, Psychopharmacology (Berl.) 236 (1) (2019) 163–182, https://doi.org/10.1007/s00213-018-5104-4.
[9] Y.D. Jeon, J.H. Lee, Y.M. Lee, D.K. Kim, Puerarin inhibits inflammation and oxidative stress in dextran sulfate sodium-induced colitis mice model, Biomed. Pharmacother. 124 (2020), 109847, https://doi.org/10.1016/j.biopha.2020.109847.
[10] Q. Liu, C. Wang, Q. Meng, J. Wu, H. Sun, P. Sun, X. Ma, X. Huo, K. Liu, Puerarin sensitized K562/ADR cells by inhibiting NF-κB pathway and inducing autophagy, Phytother. Res. 35 (3) (2021) 1658–1668, https://doi.org/10.1002/ptr.6932.

[11] T. Horn, J. Klein, Neuroprotective effects of lactate in brain ischemia: dependence on anesthetic drugs, Neurochem. Int. 62 (3) (2013) 251–257, https://doi.org/10.1016/j.neuint.2012.12.017.
[12] Z. Zhang, S. Guo, X. Cao, B. Cao, Establishment of a rat model of middle cerebral artery thrombotic ischemia, Med. J. Chin. PLA 26 (6) (2001) 423–425.
[13] E. Longa, P. Weinstein, S. Carlson, R. Cummins, Reversible middle cerebral artery occlusion without craniectomy in rats, Stroke 20 (1) (1989) 84–91, https://doi.org/10.1161/01.str.20.1.84.
[14] B. Gong, C. Li, Q. Ren, J. Li, S. Huang, An study of the "staircase test" evaluating forelimb function of rat model with focal cerebral ischemia, J. Chongqing Med. Univ. 32 (10) (2007) 1055–1058, https://doi.org/10.3969/j.issn.0253-3626.2007.10.012.
[15] J. Li, S. Guo, S. Xiao, Protective effects of curdione on cognitive and neurological function in mice with cerebral ischemia-reperfusion injury, Chin. J. Comp. Med. 30 (2) (2020) 84–89, https://doi.org/10.3969/j.issn.1671-7856.2020.02.013.
[16] C. Bertoni-Freddari, P. Fattoretti, T. Casoli, C. Spagna, W. Meier-Ruge, Morphological alterations of synaptic mitochondria during aging. The effect of Hydergine treatment, Ann. N. Y. Acad. Sci. 717 (1994) 137–149, https://doi.org/10.1111/j.1749-6632.1994.tb12081.x.
[17] M. Murahari, V. Singh, P. Chaubey, V. Suvarna, A critical review on anticancer mechanisms of natural flavonoid puerarin, Anti Cancer Agents Med. Chem. 20 (6) (2020) 678–686, https://doi.org/10.2174/1871520620666200227091811.
[18] M. Chang, Y. Tian, L. Qiao, X. Wang, Z. Di, Z. Liu, J. Mao, H. Wu, Protective effects and related mechanisms of puerarin preconditioning on focal cerebral ischemia-reperfusion injury in rats, Stroke Nervous Dis. 21 (2) (2014) 94–97, https://doi.org/10.3969/j.issn.1007-0478.2014.02.009.
[19] Y. Zhang, X. Yang, X. Ge, F. Zhang, Puerarin attenuates neurological deficits via Bcl-2/Bax/cleaved caspase-3 and Sirt3/SOD2 apoptotic pathways in subarachnoid hemorrhage mice, Biomed. Pharmacother. 109 (2019) 726–733, https://doi.org/10.1016/j.biopha.2018.10.161.
[20] L.X. Zhao, A.C. Liu, S.W. Yu, Z.X. Wang, X.Q. Lin, G.X. Zhai, Q.Z. Zhang, The permeability of puerarin loaded poly(butylcyanoacrylate) nanoparticles coated with polysorbate 80 on the blood-brain barrier and its protective effect against cerebral ischemia/reperfusion injury, Biol. Pharm. Bull. 36 (8) (2013) 1263–1270, https://doi.org/10.1248/bpb.b12-00769.
[21] S.Y. Dong, Y.J. Guo, Y. Feng, X.X. Cui, S.H. Kuo, T. Liu, Y.C. Wu, The epigenetic regulation of HIF-1α by SIRT1 in MPP(+) treated SH-SY5Y cells, Biochem. Biophys. Res. Commun. 470 (2) (2016) 453–459, https://doi.org/10.1016/j.bbrc.2016.01.013.
[22] X. Liu, A. Guo, Y. Tu, W. Li, L. Li, W. Liu, J. Ju, Y. Zhou, A. Sang, M. Zhu, Fruquintinib inhibits VEGF/VEGFR2 axis of choroidal endothelial cells and M1-type macrophages to protect against mouse laser-induced choroidal neovascularization, Cell Death Dis. 11 (11) (2020) 1016, https://doi.org/10.1038/s41419-020-03222-1.
[23] J. Xu, Y. Tu, Y. Wang, X. Xu, X. Sun, L. Xie, Q. Zhao, Y. Guo, Y. Gu, J. Du, S. Du, M. Zhu, E. Song, Prodrug of epigallocatechin-3-gallate alleviates choroidal neovascularization via down-regulating HIF-1α/VEGF/VEGFR2 pathway and M1 type macrophage/microglia polarization, Biomed. Pharmacother. 121 (2020), 109606, https://doi.org/10.1016/j.biopha.2019.109606.
[24] D.H. Mi, H.J. Fang, G.H. Zheng, X.G. Liang, Y.R. Ding, X. Liu, L.P. Liu, DPP-4 inhibitors promote proliferation and migration of rat brain microvascular endothelial cells under hypoxic/high-glucose conditions, potentially through the SIRT1/HIF-1/VEGF pathway, CNS Neurosci. Ther. 25 (3) (2019) 323–332, https://doi.org/10.1111/cns.13042.
[25] L. Geng, G. Zhang, M. Yao, Y. Fang, Rip 1-dependent endothelial necroptosis participates in ischemia-reperfusion injury of mouse flap, J. Dermatol. Sci. 97 (1) (2020) 30–40, https://doi.org/10.1016/j.jdermsci.2019.11.009.
[26] J. Ruan, L. Wang, J. Dai, J. Li, N. Wang, S. Seto, Hydroxysafflor yellow a promotes angiogenesis in rat brain microvascular endothelial cells injured by oxygen-glucose deprivation/reoxygenation(OGD/R) through SIRT1-HIF-1α-VEGFA signaling pathway, Curr. Neurovascular Res. 18 (4) (2021) 415–426, https://doi.org/10.2174/1567202618666211109104419.
[27] J. Li, E. Park, L.R. Zhong, L. Chen, Homeostatic synaptic plasticity as a metaplasticity mechanism - a molecular and cellular perspective, Curr. Opin. Neurobiol. 54 (2019) 44–53, https://doi.org/10.1016/j.conb.2018.08.010.
[28] R. Roesler, M.B. Parent, R.T. LaLumiere, C.K. McIntyre, Amygdala-hippocampal interactions in synaptic plasticity and memory formation, Neurobiol. Learn. Mem. 184 (2021), 107490, https://doi.org/10.1016/j.nlm.2021.107490.
[29] Y. Zhao, J. Wang, C. Liu, C. Jiang, C. Zhao, Z. Zhu, Progesterone influences postischemic synaptogenesis in the CA1 region of the hippocampus in rats, Synapse 65 (9) (2011) 880–891, https://doi.org/10.1002/syn.20915.
[30] L. Jin, X.M. Bo, Neuroprotection of sevoflurane against ischemia/reperfusion-induced brain injury through inhibiting GluN2A/GluN2B-PSD-95-MLK3 module, Exp. Brain Res. 239 (9) (2021) 2701–2709, https://doi.org/10.1007/s00221-021-06157-x.
[31] X. Li, Y. Wang, S. Han, Y. Sun, L. Li, Z. Liu, X.C. Zhang, Y. Liu, S.M. Zhao, H.R. Ji, Effects of puerarin on neurological function, and synaptic morphological structure and parameter of cerebral cortex in cerebral ischemia-reperfu-sion rats, Chin. J. Pathophysiol. 34 (11) (2018) 2043–2047, https://doi.org/10.3969/j.issn.1000-4718.2018.11.019.